

# Femtosecond laser-induced nitrogen fluorescence emission at different air pressures

Cite as: Phys. Plasmas **28**, 073302 (2021); <https://doi.org/10.1063/5.0049248>

Submitted: 03 March 2021 • Accepted: 26 June 2021 • Published Online: 15 July 2021

 Shuang Lin, Yun Zhang, He Zhang, et al.



View Online



Export Citation



CrossMark

## ARTICLES YOU MAY BE INTERESTED IN

[Influence of pressure on spectral broadening of femtosecond laser pulses in air](#)

Physics of Plasmas **28**, 043302 (2021); <https://doi.org/10.1063/5.0042998>

[Mechanism of snake-like propagation for positive streamers in a meandering plasma plume excited by a positively biased sinusoidal voltage](#)

Physics of Plasmas **28**, 073501 (2021); <https://doi.org/10.1063/5.0047988>

[Effect of time interval between pulses on the synthetic sound generated by repetitive nanosecond pulse discharge](#)

Physics of Plasmas **28**, 073502 (2021); <https://doi.org/10.1063/5.0050041>

Physics of Plasmas

Papers from 62nd Annual Meeting of the  
APS Division of Plasma Physics

Read now!

# Femtosecond laser-induced nitrogen fluorescence emission at different air pressures

Cite as: Phys. Plasmas **28**, 073302 (2021); doi: 10.1063/5.0049248

Submitted: 3 March 2021 · Accepted: 26 June 2021 ·

Published Online: 15 July 2021



View Online



Export Citation



CrossMark

Shuang Lin,<sup>1,2</sup>  Yun Zhang,<sup>1,2</sup> He Zhang,<sup>1,2</sup> Yunfeng Zhang,<sup>3</sup>  Mingying Chang,<sup>1,2</sup> Xiaoting Wang,<sup>1,2</sup> Anmin Chen,<sup>1,2</sup> Yuanfei Jiang,<sup>1,2,a)</sup> Suyu Li,<sup>1,2,a)</sup>  and Mingxing Jin<sup>1,2,4,a)</sup>

## AFFILIATIONS

<sup>1</sup>Institute of Atomic and Molecular Physics, Jilin University, Changchun 130012, People's Republic of China

<sup>2</sup>Jilin Provincial Key Laboratory of Applied Atomic and Molecular Spectroscopy, Jilin University, Changchun 130012, People's Republic of China

<sup>3</sup>Changchun Institute of Optics, Fine Mechanics and Physics, Chinese Academy of Science, Changchun 130033, People's Republic of China

<sup>4</sup>State Key Laboratory of Laser Propulsion and Application, Space Engineering University, Beijing 101416, People's Republic of China

<sup>a)</sup>Authors to whom correspondence should be addressed: [jiangyuanfei@jlu.edu.cn](mailto:jiangyuanfei@jlu.edu.cn); [sylee@jlu.edu.cn](mailto:sylee@jlu.edu.cn); and [mxjin@jlu.edu.cn](mailto:mxjin@jlu.edu.cn)

## ABSTRACT

In this paper, we experimentally investigate femtosecond laser-induced nitrogen fluorescence emission at different air pressures (0.1 Pa–100 kPa). The variation of nitrogen molecule ( $N_2$ ) and molecular nitrogen ion ( $N_2^+$ ) characteristic fluorescence spectral lines' intensity as a function of air pressure is observed. When the air pressure is between 10 Pa and 100 kPa, the intensity of fluorescence signals from  $N_2^+$  and  $N_2$  shows opposite variation as a function of air pressure. We deduce that dissociative recombination is the main pathway for the production of the  $C^3\Pi_u$  state of  $N_2$ . This research helps elucidate the physical emission mechanism of femtosecond laser-induced nitrogen fluorescence emission.

Published under an exclusive license by AIP Publishing. <https://doi.org/10.1063/5.0049248>

## I. INTRODUCTION

Since its first observation, femtosecond laser filamentation has been a hot research topic. Femtosecond laser technology has potential and is promising in applications, such as remote sensing of pollutants in the atmosphere,<sup>1</sup> generation of few-cycle optical pulses,<sup>2</sup> rainmaking,<sup>3,4</sup> and lightning protection.<sup>5,6</sup> Formation of a femtosecond laser filament is a nonlinear optical effect, which is a dynamic balance between self-focusing caused by optical Kerr effect and plasma defocusing caused by the multi-photon ionization of air molecules. This nonlinear phenomenon creates a long but weak plasma channel along the propagation path of femtosecond laser pulses.<sup>7,8</sup> It has been confirmed that intense femtosecond laser pulses can propagate over very long distances, reaching a few kilometers into the atmosphere.<sup>9,10</sup>

When femtosecond laser pulses propagate vertically into the atmosphere, the air pressure changes with altitude.<sup>11</sup> Therefore, the phenomenon caused by the femtosecond filament is different at different air pressures. During femtosecond laser filamentation, the ionization rate is around 0.1%, and the laser intensity is around  $5 \times 10^{13}$  W/cm<sup>2</sup>, which is independent of air pressure.<sup>9,12,13</sup> It has been reported that only when the air pressure is higher than 20 kPa can the

self-focusing effect be obvious, resulting in femtosecond laser filamentation.<sup>14</sup> The laser intensity inside a filament is high enough to cause ionization of the molecule, giving rise to the characteristic molecular fluorescence emission. However, when the air pressure is lower than 20 kPa, the self-focusing effect is counterbalanced by diffraction, and thus, no pulse collapse occurs. As a result, the laser intensity is not high enough to ionize the molecules in air, and therefore, no filament is formed,<sup>1,13,14</sup> which has been confirmed both theoretically and experimentally.<sup>13,14</sup> By adopting external focusing lens to focus laser beams, laser intensity can be high enough to ionize molecules at low air pressure due to the linear focusing effect. Once molecules are ionized, fluorescence emission occurs. We can divide femtosecond laser-induced fluorescence emission mechanism into two regimes, i.e., the filamentation regime ( $p \geq 20$  kPa) and the nonfilamentation regime ( $p < 20$  kPa). In the filamentation regime, due to the external focusing and self-focusing effects, the laser intensity within the filament is greatly enhanced; however, it is clamped to a certain value ( $5 \times 10^{13}$  W/cm<sup>2</sup>) due to the plasma defocusing effect.<sup>15</sup> In contrast, in the non-filamentation regime, the laser beam is mainly focused by an external focusing lens, and due to the weak defocusing effect (few plasmas are

generated), the laser intensity will exceed the well-known “clamped intensity,” reaching  $10^{14}$  W/cm<sup>2</sup>.<sup>16</sup>

To better understand the dynamical processes that nitrogen molecules undergo in the interaction region between the femtosecond laser and air, the mechanism of nitrogen fluorescence emission induced by the femtosecond laser has been well studied. For the formation of  $N_2^+(B^2\Sigma_u^+)$ , there are two possible schemes: one is multi-photon ionization of the inner-valence electrons of neutral nitrogen molecules induced by the femtosecond laser;<sup>17</sup> the other is ionization of  $N_2$  via a collision with an electron at high kinetic energy.<sup>18,19</sup> For the formation of  $N_2(C^3\Pi_u)$ , there are three main possible schemes: collision-excitation,<sup>18,19</sup> dissociative recombination,<sup>20</sup> and collision-assisted intersystem crossing.<sup>18</sup> In our previous work, we discuss the spatial distribution of the fluorescence induced by femtosecond laser filamentation in ambient air,<sup>22</sup> and propose that intersystem crossing is the main path for the formation of  $N_2(C^3\Pi_u)$ . However, under different experimental conditions, the main path for the formation of  $N_2(C^3\Pi_u)$  may differ. In this work, we observe the emission behavior of nitrogen fluorescence by altering the air pressure, which can affect ionization, collision between electrons, molecules and ions, population of vibrational levels of electronic states, and other dynamical processes.<sup>18,23,24</sup> When the air pressure changes, different processes take part in the generation of nitrogen fluorescence emission, which is not well explored. In addition, laser intensity shows different values and spatial distributions in filamentation and nonfilamentation regimes, which also affects the dynamic processes, making nitrogen fluorescence emission more complex. In this work, we systematically study nitrogen fluorescence emission induced by femtosecond laser pulses at different air pressures (0.1 Pa–100 kPa) and attempt to revisit the fluorescence emission mechanism.

## II. EXPERIMENTAL SETUP

The experiment is carried out using an ultrafast Ti: Sapphire laser amplifier (Coherent Libra) with a central wavelength of 800 nm and a pulse width of 50 fs at a repetition rate of 1 kHz. A schematic of the experimental setup is shown in Fig. 1. Throughout this paper, the pulse energy is 3.4 mJ. The laser beam is focused by a lens ( $L_1$ ) with a focal length of 400 mm into a cylindrical gas cavity with a length of 750 mm and a diameter of 100 mm. The air pressure in the cavity is adjusted by an air pump. The produced fluorescence signal is first collected by a lens ( $L_2$ : fused silica  $f = 75$  mm) and then guided to a spectrometer (Spectra

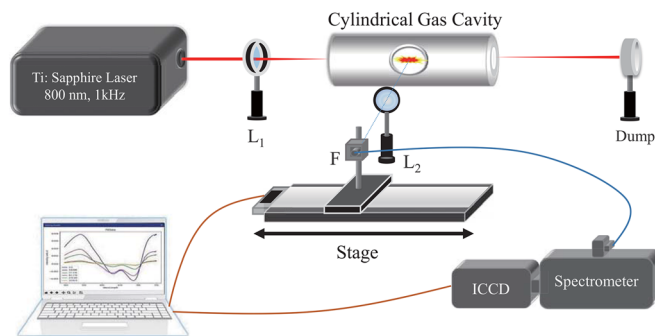


**FIG. 1.** Schematic of the experimental setup to measure the nitrogen fluorescence induced by femtosecond laser pulses at different air pressures.  $L_1$ : focusing lens with a focal length of 400 mm;  $L_2$ : fused silica lens with a focal length of 75 mm; F: optical fiber.

Pro 500i, PI Acton, with a grating of 150 grooves/mm) through a fiber on the stage. The light is detected using an intensified charge coupled device (ICCD, PI-MAX, Princeton Instruments,  $1024 \times 1024$  pixels). Since the fluorescence lifetime of nitrogen molecules can be as long as 40 ns, and that of molecular nitrogen ions as long as 67 ns at low air pressure,<sup>25</sup> in order to collect a complete fluorescence signal, the gate width is set to 100 ns. Each data point throughout this paper is typically an average of ten groups of 1000 shots' accumulation, so as to reduce the error.

## III. RESULTS AND DISCUSSION

In this paper, we are interested in fluorescence emission from nitrogen molecule ( $N_2$ ) and molecular nitrogen ion ( $N_2^+$ ). Figure 2(a) shows the typical fluorescence spectra generated during femtosecond filamentation in ambient air. Fluorescence emission from the first negative band system of  $N_2^+(B^2\Sigma_u^+ \rightarrow X^2\Sigma_g^+)$  transition and the second positive band system of  $N_2(C^3\Pi_u \rightarrow B^3\Pi_g)$  transition are observed, as shown in Fig. 2(a). In the transitions ( $v-v'$ ),  $v$  and  $v'$  denote the vibrational levels of the upper and lower electronic states, respectively.

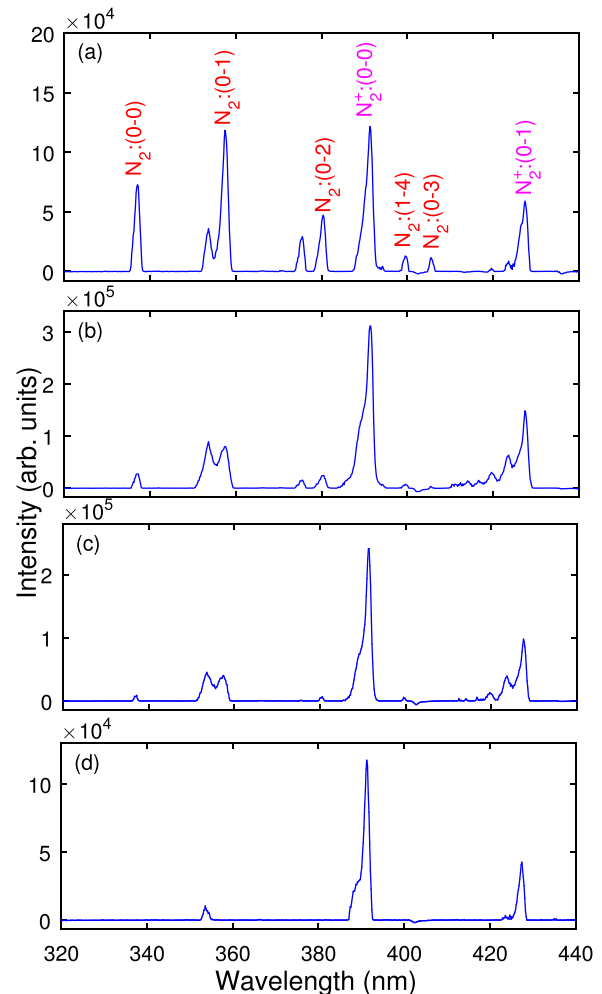


**FIG. 2.** Nitrogen fluorescence spectra induced by femtosecond laser pulse in air at (a) 100, (b) 10, (c) 1.0 kPa, and (d) 1.0 Pa.

Figure 2(d) shows that when the air pressure is low (e.g., 1.0 Pa), only the fluorescence signals from  $N_2^+$  can be observed. In this case, the molecules in the interaction region are fully ionized, meaning no nitrogen molecules now exist, and consequently, no fluorescence emission from  $N_2$  can be observed. As is known, the dynamical processes of molecules in the filamentation and nonfilamentation regimes are quite different: In the nonfilamentation regime, the number density of molecules is quite low, and thus, the proportion of ions and excited molecules is much larger in the interaction region, perhaps as high as 100%;<sup>26</sup> in contrast, in the filamentation regime, the proportion of ions and excited molecules in the interaction region is around 0.1%.<sup>27</sup> To elucidate fluorescence emission as a function of air pressure, images of side-emitted nitrogen fluorescence at different air pressures are shown in Fig. 3. In low air pressure conditions [Figs. 3(a)–3(c)], the fluorescence emitted from the interaction region of the femtosecond laser pulses and air is relatively weak. The emitted fluorescence intensity gradually increases with air pressure [Figs. 3(d)–3(f)], which is the same as the results given in Fig. 2. When we further increase the air pressure ( $p \geq 20$  kPa), it comes to the filamentation regime, and the Kerr self-focusing effect becomes stronger due to the increase in the nonlinear refractive index of air ( $n_2$ ) in the interaction region. Due to the combined action of the Kerr self-focusing effect and external focusing, the position where the fluorescence appears moves toward the entrance of the cavity, as shown by the dotted lines in Figs. 3(g)–3(i). We estimate the length of the filament in the interaction region (filamentation regime) to be about 2 cm, as shown in

Figs. 3(g)–3(i). In Figs. 3(a)–3(f), the length of the region that emits fluorescence in the interaction region (nonfilamentation regime) is about 2.2, 2.4, 2.8, 2.6, 2.1, and 2.1 cm, respectively. When the air pressure is 1 and 10 Pa [Figs. 3(a) and 3(b)], the number density of molecules is low; therefore, the length of the region that emits fluorescence is shorter. This region gets shorter with the increasing air pressure because of two main reasons: (1) with the increase in air pressure, the self-focusing effect becomes stronger, so that the focusing ability of laser pulse is enhanced. The focal point moves toward the entrance of the cavity and the light diverges faster after the focal point; (2) the total energy of the laser pulses is constant, and the energy that is consumed in the ionization of molecules at the focal point increases with the increasing air pressure. Therefore, the remaining energy used to ionize the molecules after the focal point decreases with the increasing air pressure; that is, the emitted nitrogen fluorescence after the focal point becomes weaker with the increasing air pressure.

In order to clearly show the dependence of fluorescence signals' intensity on air pressure, we choose 337 nm [ $N_2(C^3\Pi_u(\nu=0)) \rightarrow N_2(B^3\Pi_g(\nu'=0))$  transition], 380 nm [ $N_2(C^3\Pi_u(\nu=0)) \rightarrow N_2(B^3\Pi_g(\nu'=2))$  transition], 400 nm [ $N_2(C^3\Pi_u(\nu=1)) \rightarrow N_2(B^3\Pi_g(\nu'=4))$  transition], 405 nm [ $N_2(C^3\Pi_u(\nu=0)) \rightarrow N_2(B^3\Pi_g(\nu'=3))$  transition], 391 nm [ $N_2^+(B^2\Sigma_u^+(\nu=0)) \rightarrow N_2^+(X^2\Sigma_g^+(\nu'=0))$  transition], and 428 nm [ $N_2^+(B^2\Sigma_u^+(\nu=0)) \rightarrow N_2^+(X^2\Sigma_g^+(\nu'=1))$  transition] spectral lines as examples to study

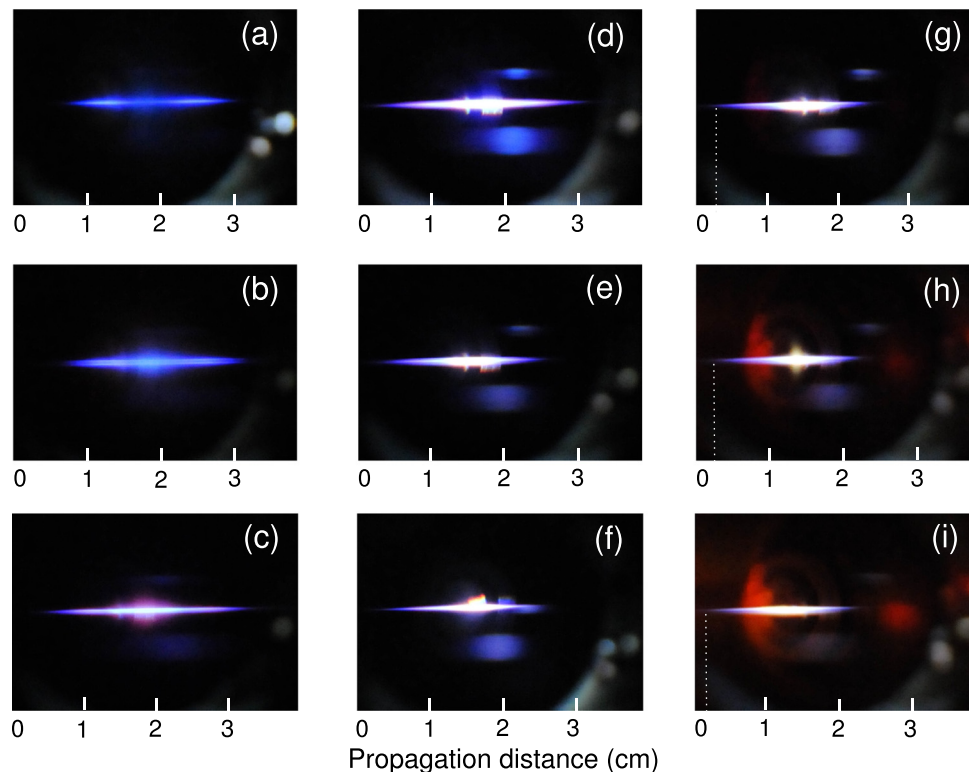


**FIG. 3.** Nitrogen fluorescence images at (a) 1, (b) 10, (c) 120, (d) 790, (e) 3500, (f) 8000 Pa, (g) 20, (h) 50, and (i) 100 kPa. The dotted lines indicate the position where fluorescence appears.



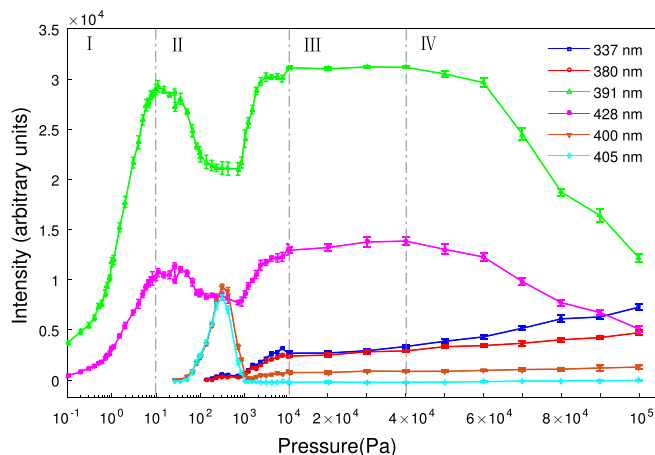


**FIG. 4.** Evolution of 337, 380, 391, 400, 405, and 428 nm spectral lines with air pressure. The error bars indicate the uncertainty of fluorescence intensity.

the fluorescence emission from  $N_2$  and  $N_2^+$ , and present the evolution of their intensity with air pressure, as shown in Fig. 4. In order to show the correlative variation between  $N_2^+$  and  $N_2$  fluorescence signals' intensity more clearly, we divide Fig. 4 into four regions (Regions I, II, III, and IV) for a detailed discussion. The intensity of  $N_2^+$  fluorescence signals at 391 and 428 nm (see the green triangles and the pink crosses in Fig. 4) increases with the increasing air pressure, reaching its maxima at around 10 Pa (Region I); the intensity of fluorescence signals first decreases and then increases when the air pressure is between 10 Pa and 10 kPa (Region II); the intensity of fluorescence signals remains constant when the air pressure is between 20 and 40 kPa (Region III); and then decreases greatly when the air pressure is higher than 40 kPa (Region IV). The intensity of  $N_2$  fluorescence signals at 337 and 380 nm (see the blue squares and red circles in Fig. 4) appears at about 100 Pa (Region II) because only a proportion of the molecules in the interaction region are ionized, and excited  $N_2$  molecules are generated, thus emitting fluorescence. The generation mechanism of  $N_2$  fluorescence emission will be discussed later. The intensity of  $N_2$  fluorescence signals at 337 and 380 nm increases slowly when the air pressure is between 20 and 40 kPa (Region III), and continuously increases when the air pressure is higher than 40 kPa (Region IV). It should be noted that the 400 and 405 nm spectral lines, which also come from  $N_2$ , appear at about 49 Pa and disappear at about 1000 Pa (see the inverted orange triangles and the cyan diamonds in Fig. 4).

It should be noted that the collision not only plays an important role in the generation of free electrons, excited molecules and ions, but also affects their dynamical processes as well as the accompanying fluorescence emission.<sup>18,19,21</sup> With respect to the fluorescence emission from molecular nitrogen ions, Becker *et al.* have confirmed that the  $B^2\Sigma_u^+$  states of  $N_2^+$  are populated by the multi-photon ionization of the inner-valence electrons of neutral nitrogen molecules induced by the femtosecond laser.<sup>17</sup> Because the number density of nitrogen molecules is directly proportional to the air pressure, if collision does not influence the dynamical processes of fluorescence emission, the number density of the excited molecular nitrogen ions generated by ionization is directly proportional to the air pressure for a given laser intensity. Consequently, the intensity of  $N_2^+$  fluorescence signals at

391 and 428 nm increases linearly with air pressure, which is contrary to the observations in Fig. 4. The generation mechanism of  $N_2$  fluorescence is still controversial, for there are three possible schemes that generate the  $C^3\Pi_u$  states of  $N_2$ : collision-induced excitation [ $N_2(X^1\Sigma_g^+) + e \rightarrow N_2(C^3\Pi_u) + e$ ],<sup>18,19</sup> collision-assisted intersystem crossing [ $N_2 + m h\nu \rightarrow N_2^*; N_2^* \xrightarrow{ISC} N_2(C^3\Pi_u)$ ],<sup>21</sup> and dissociative recombination [ $N_2^+ + N_2 \rightarrow N_4^+; N_4^+ + e \rightarrow N_2(C^3\Pi_u) + N_2$ ].<sup>18,20</sup> According to Fig. 4 (Region II and Region IV), we can see that the variation of the  $N_2^+$  fluorescence signals' intensity with air pressure is closely related to that of  $N_2$  fluorescence signals with air pressure: when the intensity of  $N_2$  fluorescence signals increases, that of  $N_2^+$  fluorescence signals decreases; conversely, when the intensity of  $N_2$  fluorescence signals decreases, that of  $N_2^+$  fluorescence signals increases. In other words, there is an anti-correlation between  $N_2^+$  and  $N_2$  fluorescence signals' intensity. It should be noted that the intensity of  $N_2$  fluorescence signals at 337 and 380 nm increases slightly when the air pressure is between 1000 and 10 000 Pa. We speculate that dissociative recombination still occurs in this air pressure range, resulting in the formation of a small amount of  $N_2(C^3\Pi_u)$ . The number density of  $N_2^+$  consumed to generate  $N_2(C^3\Pi_u)$  is not enough to affect the increase in the total number density of  $N_2^+$ . Therefore, in the overall variation of  $N_2^+$  and  $N_2$  fluorescence signals' intensity in Region II, the intensity of  $N_2^+$  and  $N_2$  fluorescence signals shows opposite variation. Among the three emission mechanisms, only dissociative recombination involves the correlative variation between the fluorescence signals from  $N_2^+$  and that from  $N_2$ . Therefore, we speculate that dissociative recombination is the best explanation for the correlative variation between the intensity of  $N_2^+$  and  $N_2$  fluorescence signals. Though the influence of collisions on  $N_2$  fluorescence emission cannot be ruled out at present, our analysis indicates that collision-excitation and collision-assisted intersystem crossing do not play major roles in the generation of the  $C^3\Pi_u$  states of  $N_2$ .

In Region I, for the 391 and 428 nm lines of  $N_2^+$ , when the air pressure increases, the lines' intensities increase rapidly and reach their maxima at around 10 Pa due to the increase in the number density of  $N_2^+$ . Region II shows that the fluorescence signals of  $N_2$  at 400 and 405 nm appear at about 49 Pa, and then their intensities increase gradually before 300 Pa. This phenomenon is likely caused by the increasing number density of  $N_2^+$  that participates in the dissociative recombination process, thereby increasing the number density of  $N_2(C^3\Pi_u)$ . At the same time, the number density of  $N_2^+$  decreases, and therefore, the intensity of  $N_2^+$  fluorescence signals at 391 and 428 nm decreases. As we further increase the air pressure, the intensity of  $N_2$  fluorescence signals at 400 and 405 nm decreases gradually and eventually disappears at about 1000 Pa. This can be attributed to the fact that dissociative recombination is weakened with increasing air pressure. As dissociative recombination weakens, the number density of  $N_2^+$  that participates in the dissociative recombination process is reduced, and the number density of  $N_2^+$  that emits fluorescence increases; as a result, the intensity of  $N_2^+$  fluorescence signals at 391 and 428 nm increases again. To clearly show the variation in  $N_2$  (400 and 405 nm lines) and  $N_2^+$  (391 and 428 nm lines) fluorescence signals' intensity at air pressures between 49 and 1000 Pa, Fig. 5 shows the nitrogen fluorescence spectra (385–432 nm) induced by a femtosecond laser pulse for this air pressure range.

It is worth noting that when the fluorescence signals of  $N_2$  at 400 and 405 nm appear (see Region II in Fig. 4), the fluorescence signals at

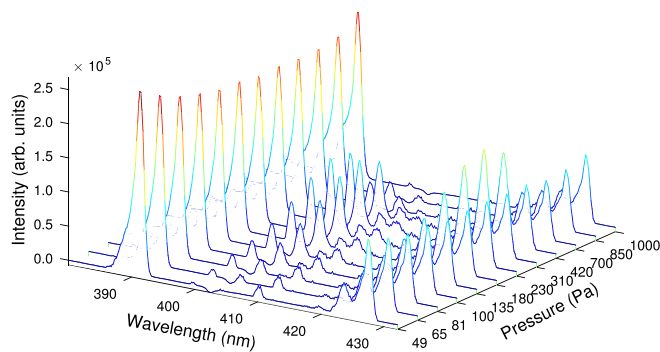


**FIG. 5.** Spectra of nitrogen fluorescence (385–432 nm) induced by a femtosecond laser pulse for air pressures ranging from 49 to 1000 Pa.

337 and 380 nm, which also originate from  $N_2$ , do not appear. The possible cause for this is that the 400, 405 nm spectral lines and 337, 380 nm spectral lines correspond to different vibrational levels of the lower electronic states (i.e.,  $B^3\Pi_g$ ) of the transition  $C^3\Pi_u \rightarrow B^3\Pi_g$ : the 400, 405 nm spectral lines correspond to the higher vibrational levels ( $v' = 4, 3$ ), and the 337, 380 nm spectral lines correspond to the lower vibrational levels ( $v' = 0, 2$ ). The population of the higher vibrational levels is reduced at higher laser intensity,<sup>23</sup> resulting in a decrease in the population of the  $B^3\Pi_g$  ( $v' = 4, 3$ ) states of  $N_2$  (the laser intensity in Region II is relatively high, about  $10^{14}$  W/cm<sup>2</sup>, due to the weak defocusing effect). The  $C^3\Pi_u$  ( $v = 0, 1$ )  $\rightarrow$   $B^3\Pi_g$  ( $v' = 3, 4$ ) transitions are more likely to occur than the  $C^3\Pi_u$  ( $v = 0$ )  $\rightarrow$   $B^3\Pi_g$  ( $v' = 0, 2$ ) transitions. Therefore, in Region II, the 400, 405 nm fluorescence signals of  $N_2$  appear, while the  $N_2$  fluorescence signals at 337 and 380 nm remain weak in intensity. When the air pressure exceeds 1000 Pa, the intensity of  $N_2$  fluorescence signals at 405 nm is almost zero, and thus, we ignore the  $N_2$  fluorescence emission at 405 nm throughout this paper. The fundamental light (800 nm) can be frequency-doubled, via a nonlinear optical effect. Therefore, the effect of frequency doubling is enhanced by increasing air pressure. We speculate that 400 nm signals are more likely to be generated from fundamental light (800 nm) after being frequency-doubled. Therefore, we also ignore 400 nm signals throughout this paper when the air pressure exceeds 1000 Pa.

In Region III, collision-assisted deactivation, in which the  $N_2^+$  collides with surrounding oxygen molecules, reduces the population of upper excited state of molecular nitrogen ions.<sup>28</sup> Since the deactivation effect is directly proportional to air pressure,<sup>29</sup> the population of excited  $B^2\Sigma_u^+$  states of  $N_2^+$  is inversely proportional to air pressure. Comprehensively, considering the combined effects of direct excitation, ionization, and collision on the generation of  $N_2^+$  fluorescence signals, the intensity of  $N_2^+$  fluorescence signals is independent of air pressure in Region III. The intensity of  $N_2$  fluorescence signals at 337 and 380 nm increases slowly in Region III. We speculate that this is because the number density of  $N_2^+$  remains nearly constant, and the number density of  $N_2(C^3\Pi_u)$  generated by dissociative recombination also remains nearly constant. The collision-induced excitation and collision-assisted intersystem crossing process may also contribute to the generation of the  $C^3\Pi_u$  states of  $N_2$ , meaning the observed

fluorescence signals' intensity of  $N_2$  at 337 and 380 nm increases slowly. When the air pressure is above 40 kPa (Region IV), the collision-assisted deactivation effect is stronger than direct excitation and ionization. Dissociative recombination continues; therefore, the intensity of  $N_2^+$  fluorescence signals at 391 and 428 nm decreases greatly under the combined influence of the deactivation effect and dissociative recombination. Meanwhile, the intensity of  $N_2$  fluorescence signals at 337 and 380 nm gradually increases with increasing air pressure. This may occur because of the increase in the number density of  $N_2^+$  that participates in the dissociative recombination process, increasing the number density of  $N_2(C^3\Pi_u)$ .

In the previous work, we concluded that the intersystem crossing scheme plays a main role in the formation of  $N_2(C^3\Pi_u)$  in ambient air.<sup>21</sup> In this work, the air pressure range of experimental conditions is 0.1 Pa–100 kPa, which covers ambient air conditions. However, according to the variation of  $N_2^+$  and  $N_2$  fluorescence signals' intensity in Region IV, we deduce that dissociative recombination is the best explanation for this variation. We are not denying the contribution of intersystem crossing to the formation of  $N_2(C^3\Pi_u)$ ; however, it only makes a minor contribution under the experimental conditions in this work. Therefore, the speculation in this work is not in contradiction with the conclusion of our previous work.<sup>21</sup>

#### IV. CONCLUSION

In this paper, we study nitrogen fluorescence emission induced by an intense femtosecond laser in air at different air pressures (0.1 Pa–100 kPa). By observing the variation of nitrogen molecule ( $N_2$ ) and molecular nitrogen ion ( $N_2^+$ ) characteristic fluorescence spectral lines' intensity with increasing air pressure, it is found that from 10 Pa to 100 kPa, the intensity of  $N_2^+$  and  $N_2$  fluorescence signals shows opposite variation as a function of air pressure. We speculate that the formation of  $N_2(C^3\Pi_u)$  states is most likely to be caused by the dissociative recombination process. Although the contribution of collision-induced excitation and collision-assisted intersystem crossing mechanisms to the generation of  $N_2(C^3\Pi_u)$  cannot be ruled out in our work, they may not play a major role. We hope this work acts as a guide to the emission mechanism of femtosecond laser-induced nitrogen fluorescence.

#### ACKNOWLEDGMENTS

This work is supported by the National Key Research and Development Program (Grant No. 2019YFA0307701), the National Natural Science Foundation of China (Grant Nos. 11704145, 11974138, 11674128, 11504129, and 11674124), and the Scientific Research Project of Jilin Provincial Department of Education during the 13th Five-year Plan Period (Grant No. JJKH20190181KJ).

#### DATA AVAILABILITY

The data that support the findings of this study are available from the corresponding author upon reasonable request.

#### REFERENCES

- Q. Luo, H. L. Xu, S. A. Hosseini, J. F. Daigle, F. Théberge, M. Sharifi, and S. L. Chin, *Appl. Phys. B* **82**, 105 (2006).
- C. P. Hauri, W. Kornelis, F. W. Helbing, A. Heinrich, A. Couairon, A. Mysyrowicz, J. Biegert, and U. Keller, *Appl. Phys. B* **79**, 673 (2004).

- <sup>3</sup>J. J. Ju, J. S. Liu, C. Wang, H. Y. Sun, W. T. Wang, X. C. Ge, C. Li, S. L. Chin, R. Li, and Z. Z. Xu, *Opt. Lett.* **37**, 1214 (2012).
- <sup>4</sup>P. Rohwetter, J. Kasparian, K. Stelmaszczyk, Z. Q. Hao, S. Henin, N. Lascoux, W. M. Nakaema, Y. Petit, M. Queißer, R. Salame, E. Salmon, L. Wöste, and J. P. Wolf, *Nat. Photonics* **4**, 451 (2010).
- <sup>5</sup>R. Ackermann, K. Stelmaszczyk, P. Rohwetter, G. Méjean, E. Salmon, J. Yu, J. Kasparian, G. Méchain, V. Bergmann, S. Schaper, B. Weise, T. Kumm, K. Rethmeier, W. Kalkner, L. Wöste, and J. P. Wolf, *Appl. Phys. Lett.* **85**, 5781 (2004).
- <sup>6</sup>S. Tzortzakis, B. Prade, M. Franco, A. Mysyrowicz, S. Hüller, and P. Mora, *Phys. Rev. E* **64**, 057401 (2001).
- <sup>7</sup>A. Couairon and A. Mysyrowicz, *Phys. Rep.* **441**, 47 (2007).
- <sup>8</sup>S. Y. Li, F. M. Guo, Y. Song, A. M. Chen, Y. J. Yang, and M. X. Jin, *Phys. Rev. A* **89**, 023809 (2014).
- <sup>9</sup>B. L. Fontaine, F. Vidal, Z. Jiang, C. Y. Chien, D. Comtois, A. Desparois, T. W. Johnston, J. C. Kieffer, and H. Pepin, *Phys. Plasmas* **6**, 1615 (1999).
- <sup>10</sup>G. Mechain, C. D'Amico, Y. B. Andre, S. Tzortzakis, M. Franco, B. Prade, A. Mysyrowicz, A. Couairon, E. Salmon, and R. Sauerbrey, *Opt. Commun.* **247**, 171 (2005).
- <sup>11</sup>M. Rodriguez, R. Bourayou, G. Mejean, J. Kasparian, J. Yu, E. Salmon, A. Scholz, B. Stecklum, J. Eisloffel, U. Laux, A. P. Hatzes, R. Sauerbrey, L. Wöste, and J. P. Wolf, *Phys. Rev. E* **69**, 036607 (2004).
- <sup>12</sup>S. Champeaux and L. Bergé, *Opt. Lett.* **31**, 1301 (2006).
- <sup>13</sup>A. Couairon, M. Franco, G. Méchain, T. Olivier, B. Prade, and A. Mysyrowicz, *Opt. Commun.* **259**, 265 (2006).
- <sup>14</sup>G. Méchain, T. Olivier, M. Franco, A. Couairon, B. Prade, and A. Mysyrowicz, *Opt. Commun.* **261**, 322 (2006).
- <sup>15</sup>J. Kasparian, R. Sauerbrey, and S. L. Chin, *Appl. Phys. B* **71**, 877 (2000).
- <sup>16</sup>S. Mitryukovskiy, Y. Liu, P. Ding, A. Houard, and A. Mysyrowicz, *Opt. Express* **22**, 12750 (2014).
- <sup>17</sup>A. Becker, A. D. Bandrauk, and S. L. Chin, *Chem. Phys. Lett.* **343**, 345 (2001).
- <sup>18</sup>S. Mitryukovskiy, Y. Liu, P. Ding, A. Houard, A. Couairon, and A. Mysyrowicz, *Phys. Rev. Lett.* **114**, 063003 (2015).
- <sup>19</sup>Y. Itikawa, *J. Phys. Chem. Ref. Data* **35**, 31 (2006).
- <sup>20</sup>H. L. Xu, A. Azarm, J. Bernhardt, Y. Kamali, and S. L. Chin, *Chem. Phys.* **360**, 171 (2009).
- <sup>21</sup>B. R. Arnold, S. D. Roberson, and P. M. Pellegrino, *Chem. Phys.* **405**, 9 (2012).
- <sup>22</sup>J. B. Wu, Z. Y. Wu, T. Chen, H. Zhang, Y. F. Zhang, Y. Zhang, S. Lin, X. M. Cai, A. M. Chen, Y. F. Jiang, S. Y. Li, and M. X. Jin, *Opt. Laser Technol.* **131**, 106417 (2020).
- <sup>23</sup>T. K. Kjeldsen and L. B. Madsen, *Phys. Rev. Lett.* **95**, 073004 (2005).
- <sup>24</sup>Y. Liu, Y. Brelet, G. Point, A. Houard, and A. Mysyrowicz, *Opt. Express* **21**, 22791 (2013).
- <sup>25</sup>R. F. Wuerker, L. Schmitz, T. Fukuchi, and P. Straus, *Chem. Phys. Lett.* **150**, 443 (1988).
- <sup>26</sup>S. F. Zhao, L. Liu, and X. X. Zhou, *Opt. Commun.* **313**, 74 (2014).
- <sup>27</sup>A. Couairon and A. Mysyrowicz, *Progress in Ultrafast Intense Laser Science* (Springer, 2006).
- <sup>28</sup>S. T. Amimoto, A. P. Force, R. G. Gulotty, Jr., and J. R. Wiesenfeld, *J. Chem. Phys.* **71**, 3640 (1979).
- <sup>29</sup>F. J. Comes and F. Speier, *Z. Naturforsch.* **26a**, 1998 (1971).